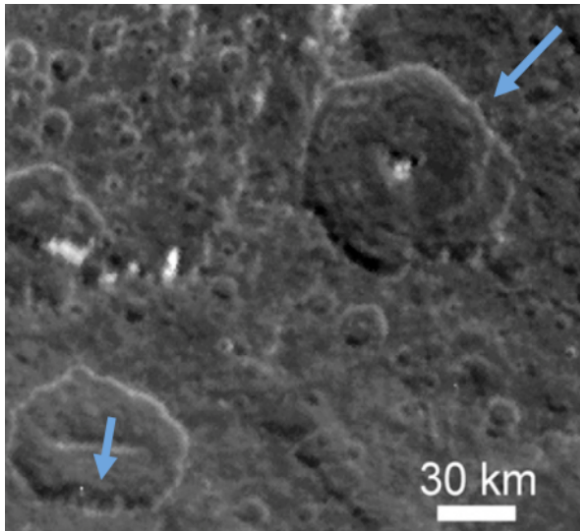


### INVESTIGATING HIDDEN FRACTURES ON IAPETUS USING POLYGONAL IMPACT CRATERS.

Chloe B. Beddingfield<sup>1,2</sup>, Richard J. Cartwright<sup>1</sup>, D. Alex Patthoff<sup>3</sup>, Ross Beyer<sup>1,2</sup>, Jeff Moore<sup>2</sup>, <sup>1</sup>The SETI Institute, Mountain View, CA 94043, chloe.b.beddingfield@nasa.gov, <sup>2</sup>NASA Ames Research Center, Moffett Field, CA 94035, <sup>3</sup>Planetary Science Institute, Tucson, AZ 85719.

**Introduction:** The surface of Iapetus exhibits an extreme albedo dichotomy between its leading and trailing hemispheres, a tidal bulge consistent with a different spin rate in the past, a large equatorial ridge, and an inclined orbit [e.g., 1]. Iapetus' inclined orbit and tidal bulge point toward unknown orbital event(s) in the past that would have generated global-scale stresses across its surface. For example, Iapetus may have experienced true polar wander after large impact events formed Engelier, Falsaron, and Turgis basins, possibly aligning these large impact craters near Iapetus' axis of spin. Furthermore, Iapetus might have experienced despinning of its rotation rate [e.g., 2]. These and other orbital events have distinct 'tectonic signatures' that can be analyzed using global stress patterns [e.g., 3].



**Figure 1:** Examples of apparent polygonal impact craters (PICs) on Iapetus [e.g., 1,4]. This figure was originally presented in [4], showing Cassini ISS image N1483173746. The blue arrows show some of the straight rim segments of apparent PICs.

However, many faults and fractures that reveal these stress patterns may have been buried by Iapetus' regolith, dust from Phoebe, and/or are below the spatial resolution of the available images, thereby limiting investigation of these stress patterns. Previous work that utilized visible tectonic features determined that Iapetus does not display a sufficient number of visible fractures to test the possible global stress mechanisms that may have modified its surface [4].

These different orbital events would each produce a unique stress pattern across the surface of Iapetus [e.g., 3]. However, prior work has not found conclusive evidence for despinning, based on the analysis of linear

tectonic features and comparison to global stress models expected for a despinning event. Evidence for other orbital events, including possible true polar wander, have not been previously investigated.

**Objective:** We are investigating these global stress events through the quantitative identification and analysis of polygonal impact craters (PICs), which are craters with at least one straight rim segment (**Figure 1**), to identify "inferred" faults and fractures on Iapetus.

**Identifying PICs:** We are identifying PICs on Iapetus by using a series of statistical tests to analyze rim azimuth distributions for each crater [5, 6]. We first manually trace the crater rim, which is normalized to the pixel length of the image used, so that each rim azimuth is associated with an equal length in the resulting distribution. We then test for a uniform azimuth distribution of each impact crater rim by applying the Pearson's Chi-Squared test. A subsequent Kolmogorov-Smirnov test is then applied to exclude degraded CICs that may be falsely classified as PICs due to non-uniform rim azimuth distributions.

Typically, fractures form in sets with consistent azimuths from fracture to fracture, which may be reflected by overprinting PICs. Therefore, PICs formed by interaction with tectonic fractures would exhibit rim azimuth distributions similar to other PICs nearby, which also reflect the same fracture azimuths. To exclude degraded CICs, we use the Kolmogorov-Smirnov test, which tests for similarity between distributions of two sets of data. The prominent rim azimuth(s) is then determined for all remaining PIC candidates. The prominent rim azimuth(s) of each crater is reflected by the mode(s) of the rim azimuth distributions. Because PICs may exhibit geometries that reflect multiple sets of controlling fractures with various azimuths, the modality, either unimodal or multimodal, of the rim azimuth distribution for each PIC candidate is determined using the Dip test.

The collections of crater rim azimuth modes for each study location is then analyzed. Over distances similar to the inter-crater distances within study locations, azimuths of fractures vary by approximately 5° to 10° [e.g., 5]. To group PIC candidates with similar azimuths, a value of 10° was used as a threshold difference between crater rim modes of PICs within a study location. If a PIC candidate in a study location exhibits a rim azimuth mode within 10° of another PIC candidate, then both craters are classified as PICs, otherwise the crater is classified as a CIC.

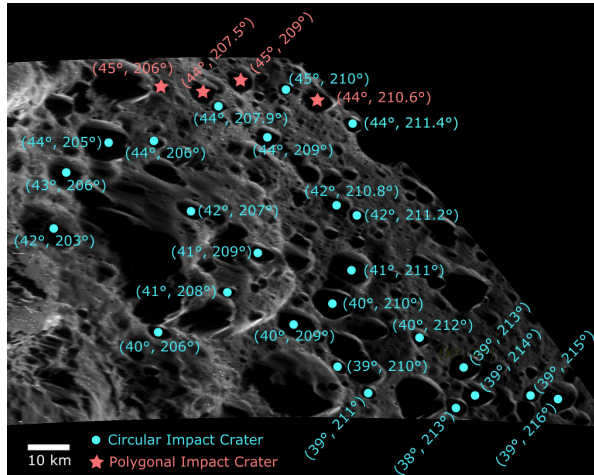


**Figure 2:** Craters analyzed in Cassini ISS image N1568121240\_2 with a resolution of 82 m/px.

**Preliminary Results:** We have identified and analyzed six PICs on Iapetus so far (**Figures 2 and 3**) and determined the orientations of some inferred fractures. We have also derived stress maps, including those estimated for diurnal tides and true polar wander (see Patthoff et al., 2022 abstract, presented at this conference).

Many impact craters on Iapetus' equatorial ridge have been overprinted by mass wasting features (**Figure 4**). The presence of these craters indicates that landslides have occurred in this region, as previously investigated by [7], and supports the interpretation that Iapetus' equatorial ridge is made up of unconsolidated material, which may have originated from a collapsed disk of ring material [e.g., 8-12]. The absence of PICs in this region further supports the interpretation that Iapetus' equatorial ridge formed via exogenic processes instead of tectonism, by indicating that subtle or subregolith fractures that we would expect with a tectonic origin are not present in this area. Furthermore the large number of craters that appear cut by mass wasting features further support the interpretation that the ridge is ancient.

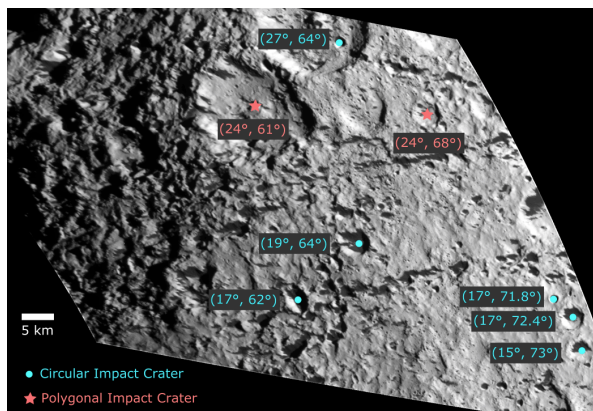


**Figure 3:** Craters analyzed in Cassini ISS image N1568137456\_2 with a resolution of 146 m/px.

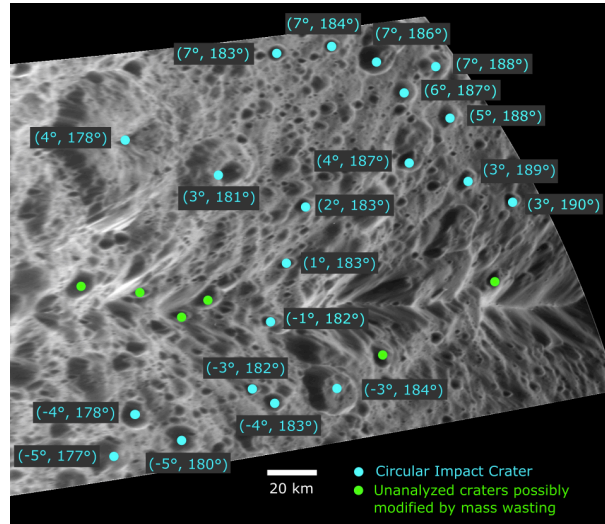


**Figure 4:** Craters analyzed in Cassini ISS image W1568126253\_1 with a resolution of 163 m/px.

**Future Work:** We will continue to identify and analyze PICs on Iapetus to investigate previously undiscovered tectonized regions and quantify PIC straight rim segment orientations to develop a global fracture map of Iapetus. We will then continue to generate stress maps to test the following geologic events: spin-up, despinning, orbital recession, orbital decay, true polar wander, and stresses from obliquity. We will statistically compare globally mapped PIC azimuths to derived stress maps to determine the spatial distributions and orientations of fractures, thereby revealing important clues about Iapetus' geologic history. We are also investigating the composition of Iapetus in order to better understand the dark material that may have buried some of the inferred fractures (see Cartwright et al., 2022 abstract, presented at this conference).

**Acknowledgements:** This project is funded by NASA Cassini Data Analysis Program (CDAP) grant 80NSSC21K0537.

**References:** [1] Porco, C. C. et al. (2005) *Science*, 307, 1237-1242. [2] Castillo-Rogez, J. C. et al. (2007) *Icarus*, 190, 179-202. [3] Collins, G. C. et al. (2009) *Cambridge U. Press*, Planetary Tectonics. [4] Singer, K. N. and McKinnon W. B. (2011) *Icarus*, 216, 198-211. [5] Beddingfield, C. B. et al. (2016) *Icarus*, 274, 163-194. [6] Beddingfield, C. B. and Cartwright, R. J. (2020) *Icarus*, 343, 113687. [7] Singer, K. N. et al. (2012) *Nature Geos.*, 5, 574-578. [8] Dombard, A. J. et al. (2012) *J. Geophys. Res. Plan.*, 117. [9] Ip, W. H. (2006) *Geophys. Res. Lett.*, 33. [10] Levison, H. F. et al. (2011) *Icarus*, 214, 773-778. [11] Damptz, A. L. et al. (2018) *Icarus*, 302, 134-144. [12] Detelich, C. E. et al. (2021) *Icarus*, 367, 114559.